Supplementary Information

A Novel FN-MdV Pathway and Its Role in Cerebellar Multimodular Control of Sensorimotor Behavior

Xiaolu Wang[1], **Si-yang Yu**[1], **Zhong Ren**[1], **Chris I. De Zeeuw**[1,2*], **Zhenyu Gao**[1*]

[1] Department of Neuroscience, Erasmus MC, Westzeedijk 353, 3015 AA, Rotterdam, the Netherlands

[2] Netherlands Institute for Neuroscience, Royal Dutch Academy of Arts & Science, 1105 BA, Amsterdam, the Netherlands

* email: c.dezeeuw@erasmusmc.nl; z.gao@erasmusmc.nl

Figure S1

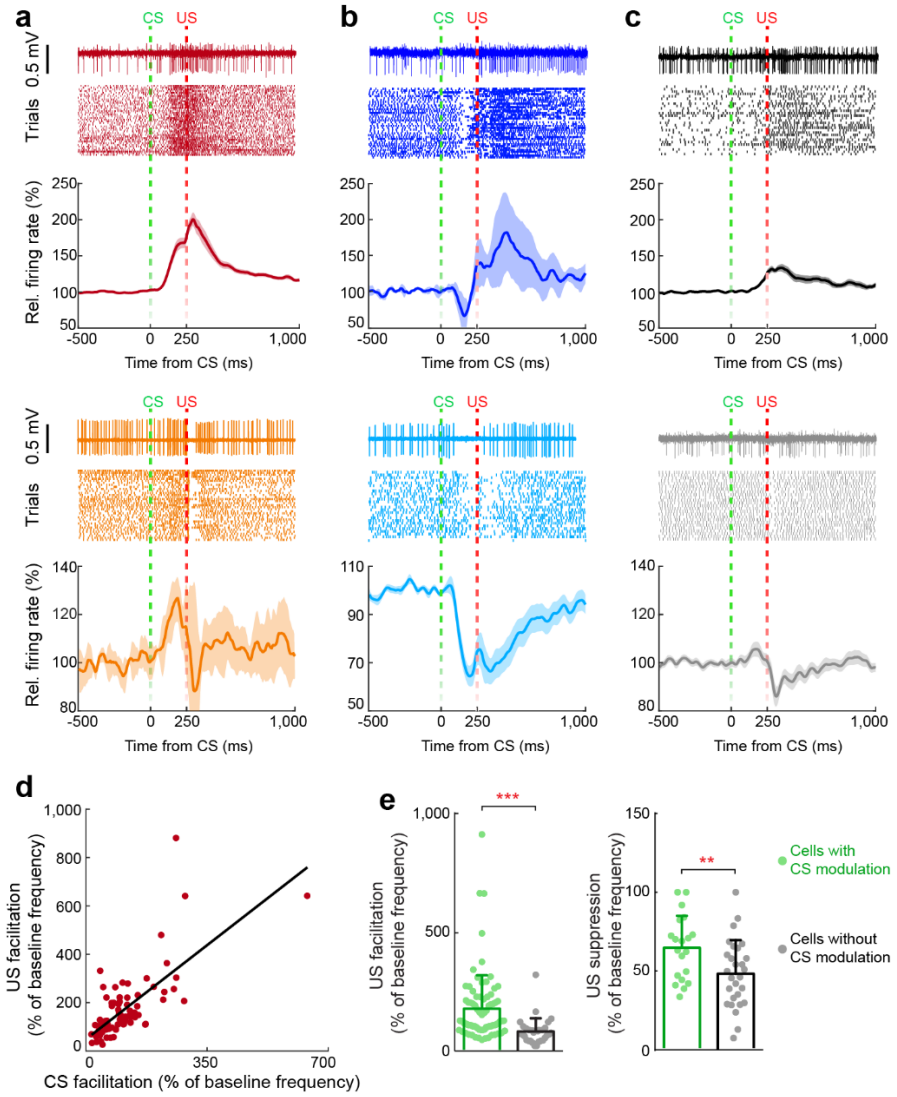

Supplementary Figure 1. US-related modulation in FN neurons. Data related to Fig. 1

a, US-related facilitation (top red panel, *n* = 80 neurons) and suppression (bottom orange panel, *n* = 6 neurons) in FN neurons exhibiting CS-related facilitation. In each panel, top row: example recording of a single trial from a representative cell; middle row: raster plot of spike events of the same cell; bottom row: group summary of spike modulation of all neurons with US-related facilitation. **b**, **c**, Same as **a**, but for the US-related modulations in FN neurons exhibiting CS-related suppression (**b**; upper dark blue: *n* = 3, lower light blue: *n* = 13) and no significant modulation (**c**; upper black: *n* = 31, lower gray: *n* = 29). **d**, Correlation between the CS- and US-related facilitation for neurons in the (**a**) red group ($P = 1.4\times10^{-13}$, $r^2 = 0.5$). **e**, Summary of the US-

related modulation (left: facilitation, n = 113; right: suppression, n = 49) in the FN neurons with and without CS-related modulation (***P < 0.001, **P < 0.01, paired t-test).

Figure S2

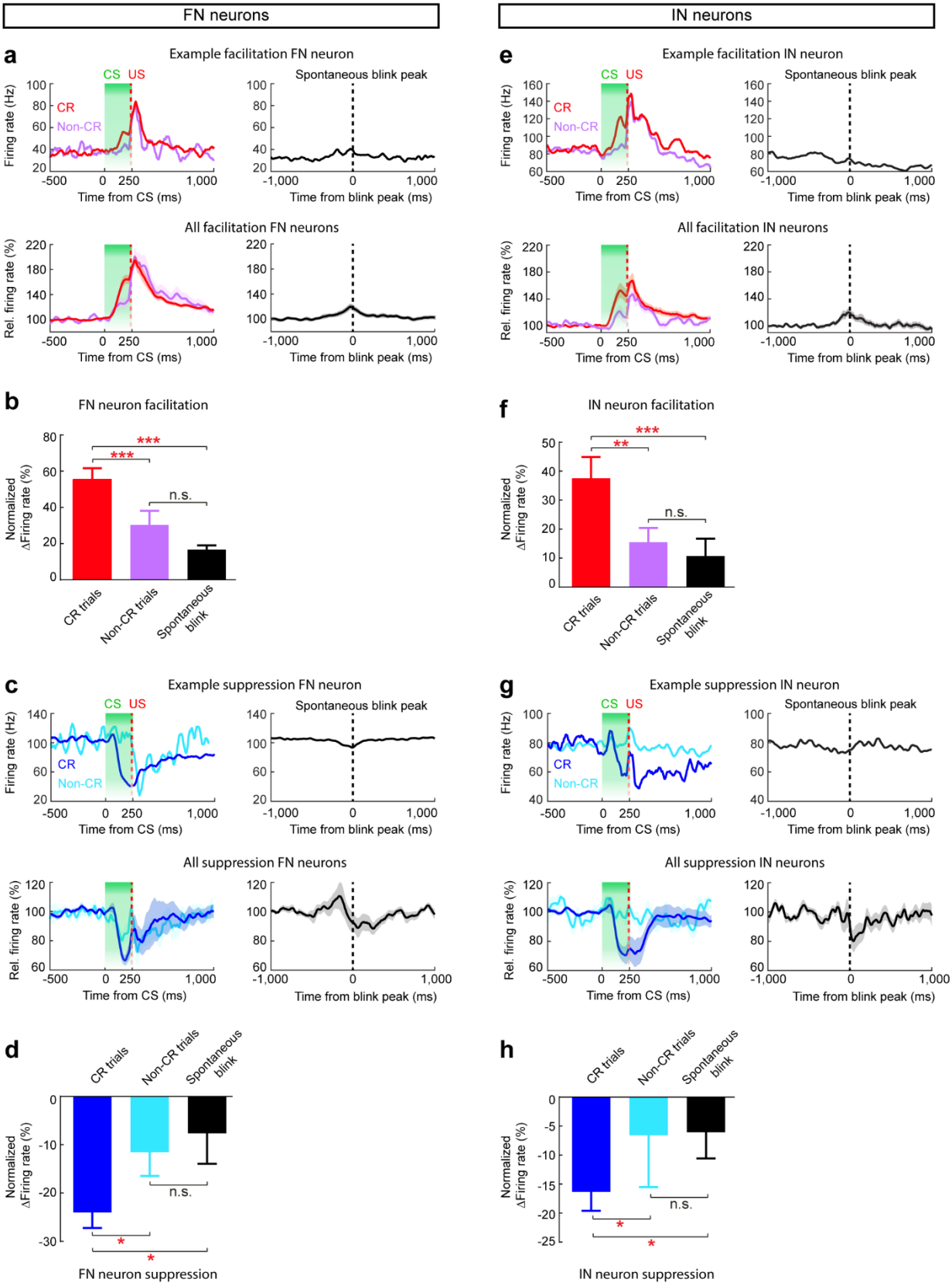
FN neurons
IN neurons
a
Example facilitation FN neuron
CS US
CR
Non-CR
Firing rate (Hz)
Time from CS (ms)
Spontaneous blink peak
Time from blink peak (ms)
All facilitation FN neurons
Rel. firing rate (%)
b
FN neuron facilitation
Normalized ΔFiring rate (%)
***
***
n.s.
CR trials
Non-CR trials
Spontaneous blink
c
Example suppression FN neuron
All suppression FN neurons
d
FN neuron suppression
n.s.
*
*
e
Example facilitation IN neuron
All facilitation IN neurons
f
IN neuron facilitation
***
**
n.s.
g
Example suppression IN neuron
All suppression IN neurons
h
IN neuron suppression
n.s.
*
*

Supplementary Figure 2. FN and IN neuron activity during non-CR trials and spontaneous blink. Data related to Fig. 1

a, FN neuron activity in CR trials (red), non-CR trials (magenta) and spontaneous blink (black). Upper: spike rates of an example neuron showing significant facilitation in CR trials, but not in non-CR trials or spontaneous blink; Lower: population average of all facilitation neurons in CR trials, non-CR trials and spontaneous blink (n = 86). **b**, Comparison of the neuron activity in CR trials, non-CR trials (during 50-250 ms after CS onset) and spontaneous blink (within 100 ms before and after spontaneous blink peak), confirming that FN neuron facilitation is CR-related. **c,d**, Same as **a,b**, but for FN neuron suppression in CR trials (blue), non-CR trials (cyan) and spontaneous blink (black). Upper: an example neuron; Lower: all suppression neurons (n = 16). **e-h**, Same as **a-b**, but for IN neurons. Dataset was also shown in our previous work (first dataset, M. Ten Brinke, *et al.*, 2017, eLife), n = 30 for facilitation IN neurons, and n = 16 for suppression IN neurons.

Figure S3

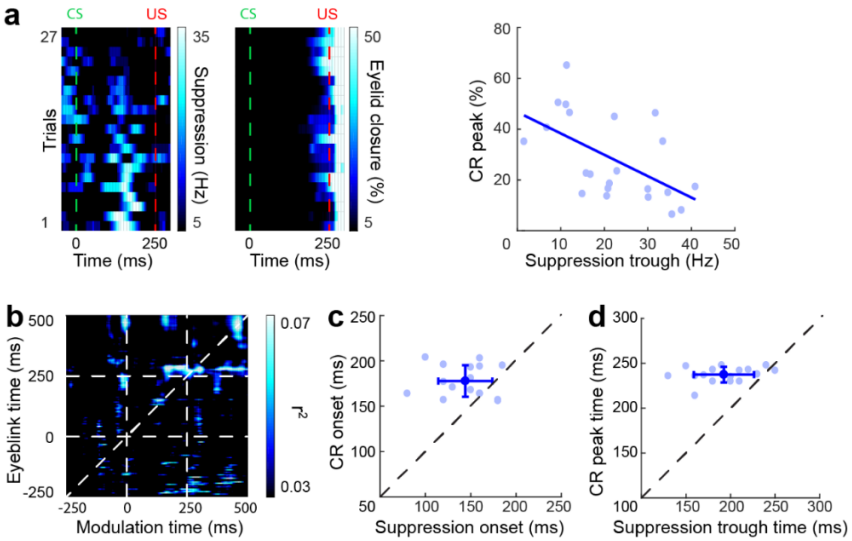

Supplementary Figure 3. Trial-by-trial correlation between FN suppression and CR amplitudes, Data related to Fig. 1

a, Example FN neuron with a trial-by-trial correlation between suppression and CR peak amplitudes. Left: Each row on the left heatmap represents a single trial of recording, and on the right heatmap represents the corresponding CR amplitudes of the same trials. All trials are ordered based on their suppression amplitudes. Dashed lines indicate CS and US onsets. Right: each dot represents a single trial; a negative correlation between neuron suppression and CR amplitudes of this cell (Linear regression model, $P < 0.01$). **b**, Average correlation matrix of 16 suppression cells. Each epoch indicates the mean r^2 value of trial-by-trial correlation between the FN neuron activity and eyelid closure at a given time point throughout the task. All epochs are minimally-correlated (dark pixels) within the CS-US interval. CS and US onsets are denoted with dashed lines in both dimensions. **c**, Relationship between the onset timings of neuronal modulation and the CR for all suppression cells, note the neuronal modulation occurred earlier than CR onset (paired *t*-test, $P < 0.01$). **d**, Same as **c**, but for the comparison of the peak timing of neuronal modulation and the trough timing of CR for all suppression cells (paired *t*-test, $P < 0.001$).

Figure S4

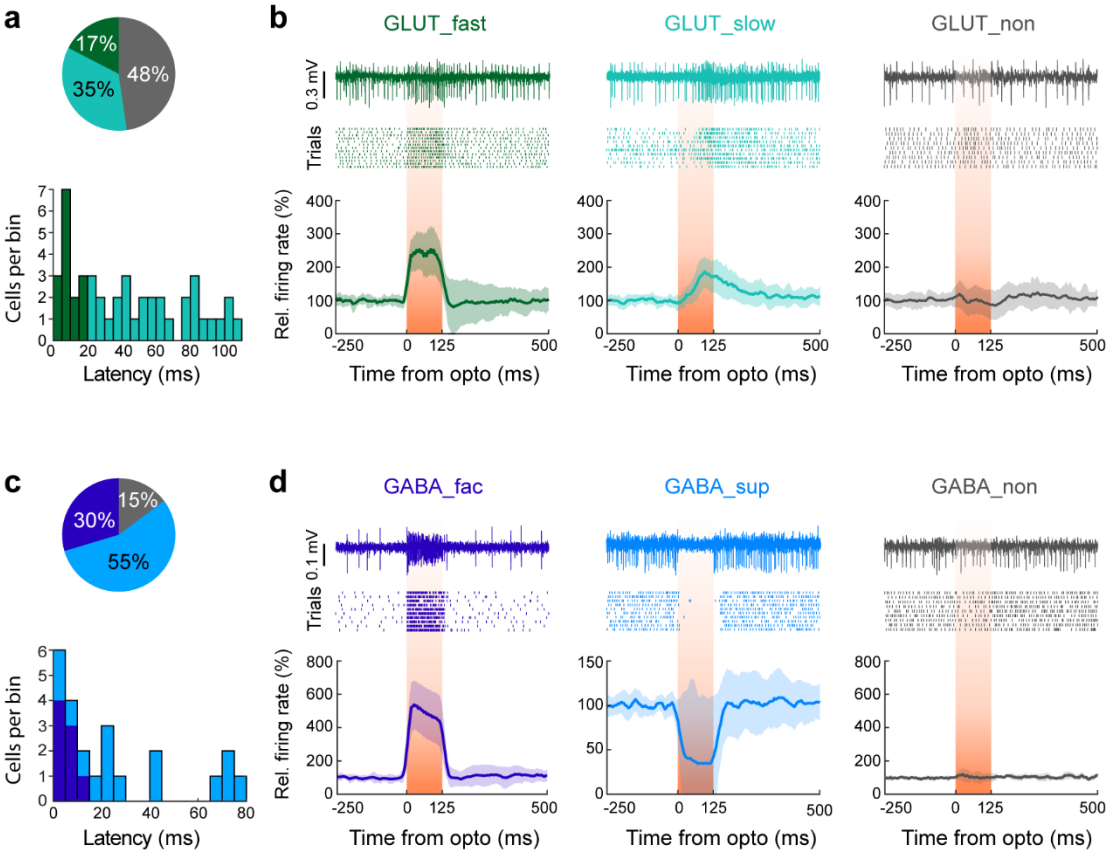

Supplementary Figure 4. FN neuron responses to optogenetic activation in VGluT2-Cre and Gad2-Cre mice. Data related to Fig. 2

a, Quantification of the facilitation latency in response to optogenetic activation of ChrimsonR in the FN neurons, in which ChrimsonR was expressed specifically in the VGluT2-cre+ cells. Summary of the fraction (upper) and the numbers of FN neurons (lower) in the VGluT2-Cre mice showing short-latency facilitation (onset < 20 ms, dark green), long-latency facilitation (onset ≥ 20 ms, light green) and no modulation (gray). **b**, Different neuron responses to the optogenetic activation in the VGluT2-Cre mice. From left to right: neuron responses to the optic light (orange shading) with short-latency facilitation (GLUT_fast, n = 15), long-latency facilitation (GLUT_slow, n = 30) and no modulation (GLUT_non, n = 41). Top row: example traces of single optogenetic stimulation trial; middle row: raster plot of spike events for each representative cell; bottom row: average neural activity of each group. **c**, Same as **a**, but for cells with short-latency facilitation (onset < 20 ms, dark blue) and suppression (light blue) in the Gad2-Cre mice. **d**, Same as **b**, but for the recordings from Gad2-Cre mice. From left to right: neuron responses to optogenetics with

short-latency facilitation (GABA_fac, *n* = 8), suppression (GABA_sup, *n* = 15) and no modulation (GABA_non, *n* = 4).

Figure S5

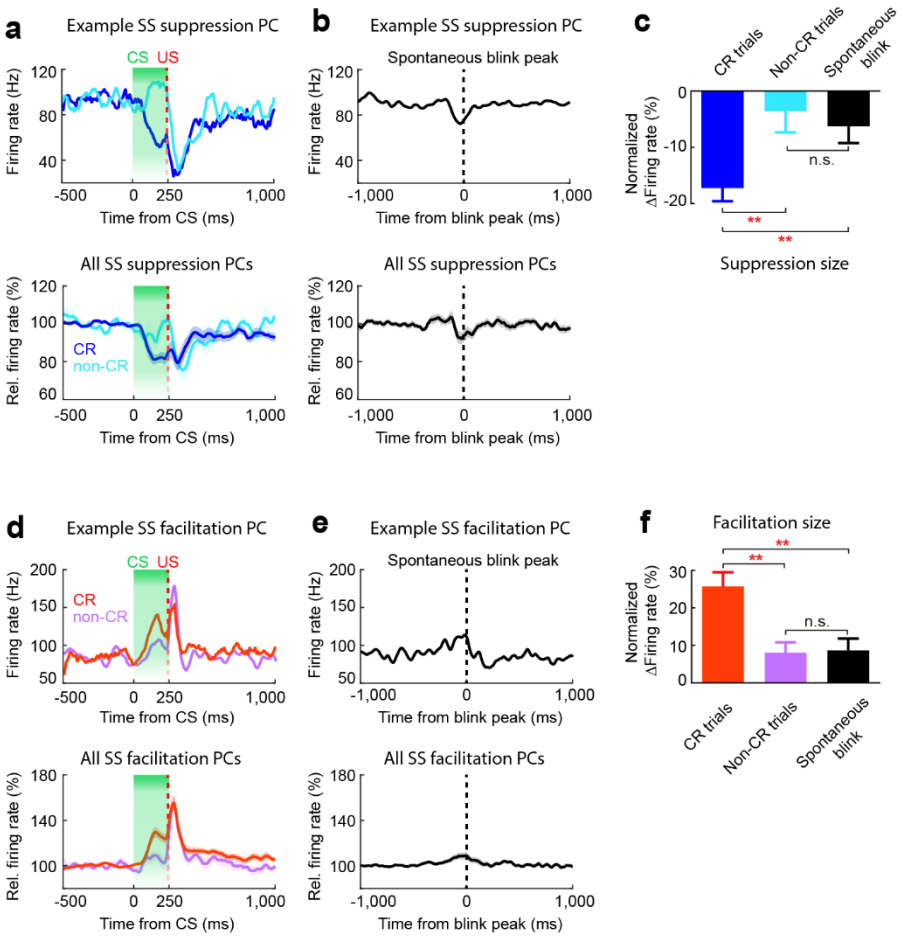

Supplementary Figure 5. Simple spike activity of vermal PCs in CR trials, non-CR trials and spontaneous blink. Data related to Fig. 3

a, Vermal PC show prominent simple spike suppression (SS suppression) in CR trials but not in non-CR trials. Upper: an example PC showing significant SS suppression in CR trials but not in non-CR trials; Lower: population activity of all SS suppression PCs (*n* = 23). **b**, SS modulation of PCs during spontaneous blink. Upper: the same example PC as in **a**, showing no significant change of firing rate during spontaneous blink; Lower, population activity of all SS suppression PCs (*n* = 23). Neuron activity is aligned to the peak of spontaneous blinking events. **c**, Summary of the SS suppression during CR trials, non-CR trials (during 50-250 ms after CS onset) and spontaneous blink (within 100 ms before and after spontaneous blink peak). **d-f**, Same as **a-c**, but for vermal PCs with simple spike facilitation (SS facilitation). Upper: an example PC; Lower: all PCs with SS facilitation (*n* = 26). ** p< 0.01.

Figure S6

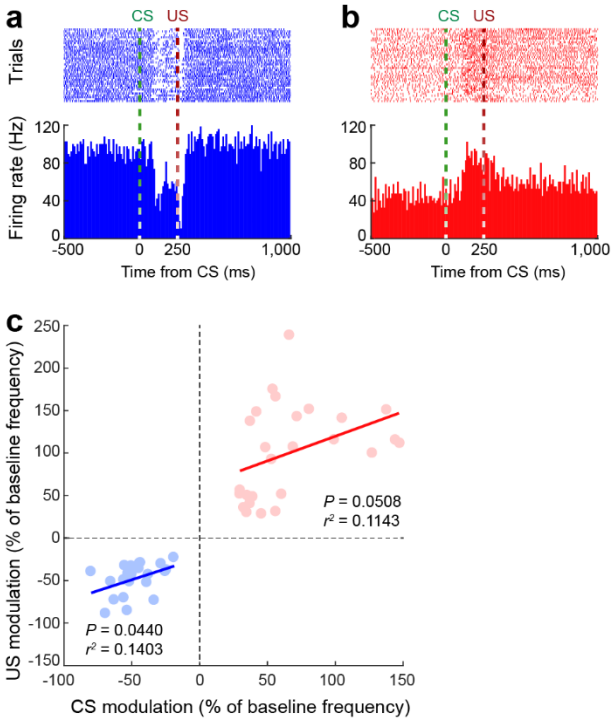

Supplementary Figure 6. US-related simple spike modulation in vermal PCs. Data related to Fig. 3

a, **b**, Raster plots of simple spikes (top) and corresponding PSTHs (bin size = 5 ms) of two example PCs showing suppression (**a**) and facilitation (**b**) in response to US. **c**, Correlation between CS- and US-related modulation (Linear model regressions). Red dots denote cells with US-related facilitation, and blue dots denote cells with US-related suppression.

Figure S7

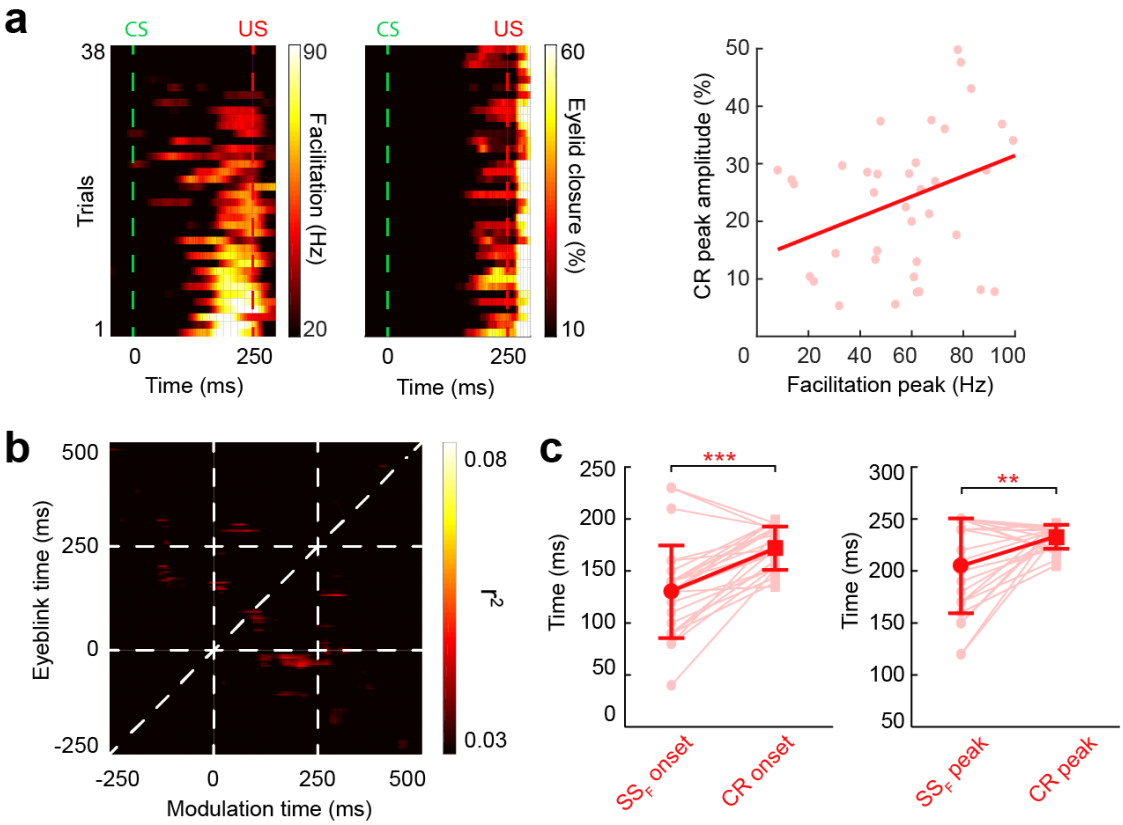

Supplementary Figure 7. Trial-by-trial correlation between simple spike facilitation and CR amplitudes, Data related to Fig. 3

a, Left panel, example PC with a positive correlation between simple spike activity and CR amplitudes. Each row on the left heatmap represents a single trial of recording, and on the right heatmap represents the corresponding CR amplitude of the same trial. Trials are ordered based on the facilitation peak amplitude. Dashed lines indicate the CS and US onsets. Right panel, positive correlation between the facilitation peak and the CR peak amplitude of the example cell (Linear regression model, $P < 0.01$). **b**, Averaged correlation matrix of all 26 PCs with simple spike facilitation. Each epoch indicates the mean r^2 value of trial-by-trial correlation between the simple spike activity and the eyelid closure at a given time point throughout the task. No significant correlation is detected within the CS-US interval (dark pixels). CS (0 ms) and US (250 ms) onsets are denoted with dashed lines in both dimensions. **c**, Comparison between the timings of simple spike facilitation and the timings of CR. Simple spike facilitation precedes behavior in both the onset (left, paired *t*-test, ***$P < 0.001$) and peak timing (right, paired *t*-test, **$P < 0.01$).

Figure S8

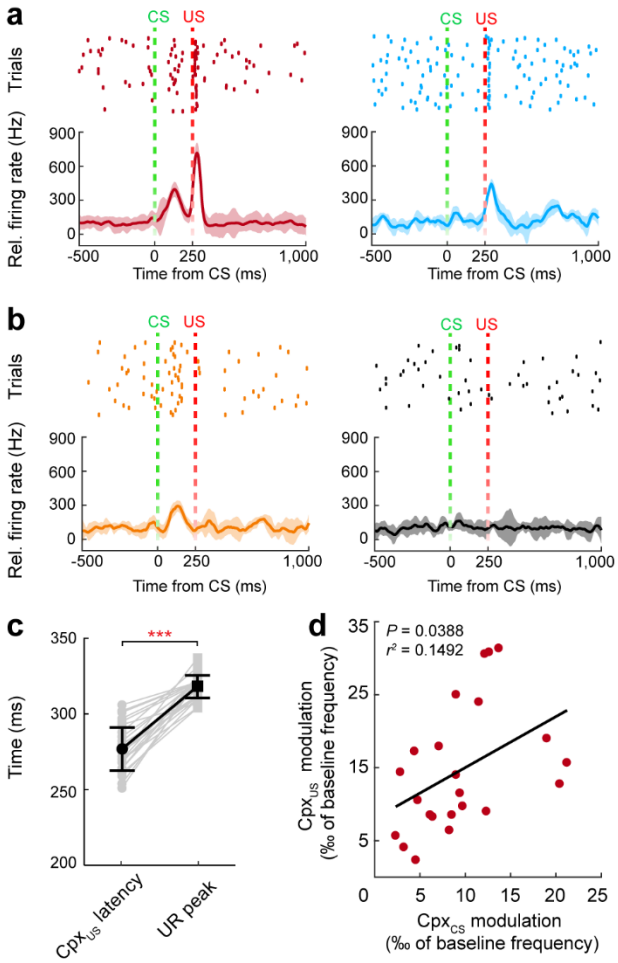

Supplementary Figure 8. US-related complex spike modulation in vermal PCs. Data related to Fig. 4

a, Short-latency US-related complex spikes (Cpx_{US}) in PCs exhibiting CS-related complex spikes (Cpx_{CS}, left red traces, n = 23 neurons) and no Cpx_{CS} (right blue traces, n = 6 neurons). Top: raster plots of complex spike events of two example cells; bottom: group average complex spike activity for each type of cells. **b**, Same as **a**, but for PCs without Cpx_{US}. **c**, Comparison of the Cpx_{US} latency and the UR peak time (paired t-test, ***P < 0.001, n = 29 neurons). **d**, Correlation between CS- and US-related complex spike modulation in the PCs of (**a**, left).

Figure S9

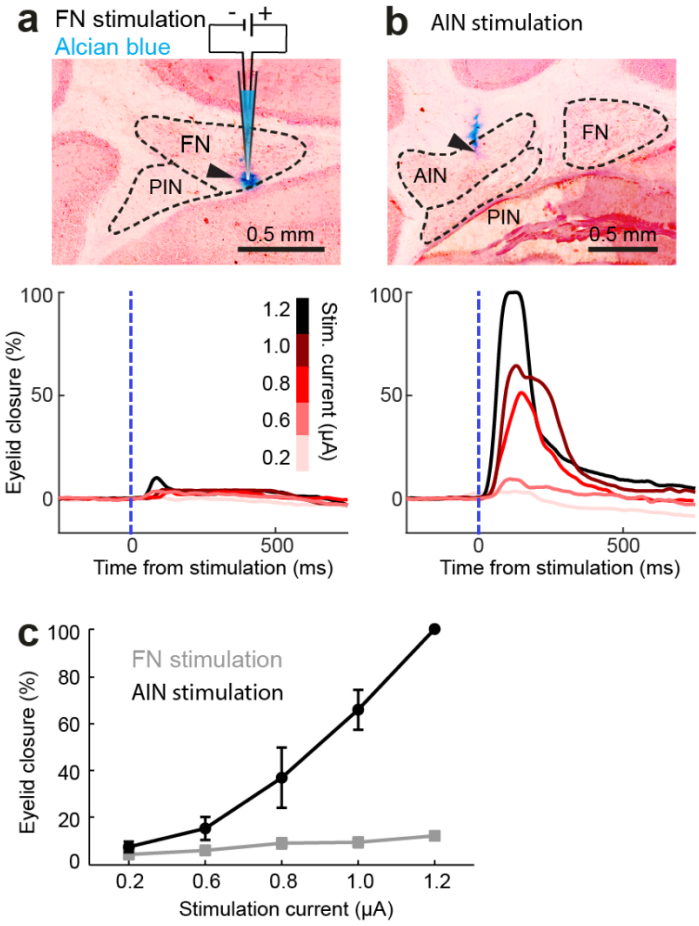

Supplementary Figure 9. Effects of electric stimulation in FN or AIN on eyelid movement. Data related to Fig. 5

a, **b**, Example histological sections showing the locations of electric stimulation in FN or AIN (upper panels) and the corresponding evoked eyelid closure with graded current intensities (lower panels) in naïve mice. Alcian blue was injected through the stimulation glass pipette to visualize the stimulation sites. **c**, Summary of eyelid closure amplitudes with different stimulation intensities in FN and AIN from 3 animals (mean ± s.e.m.). AIN: anterior interposed nucleus; PIN: posterior interposed nucleus; FN: fastigial nucleus.

Figure S10

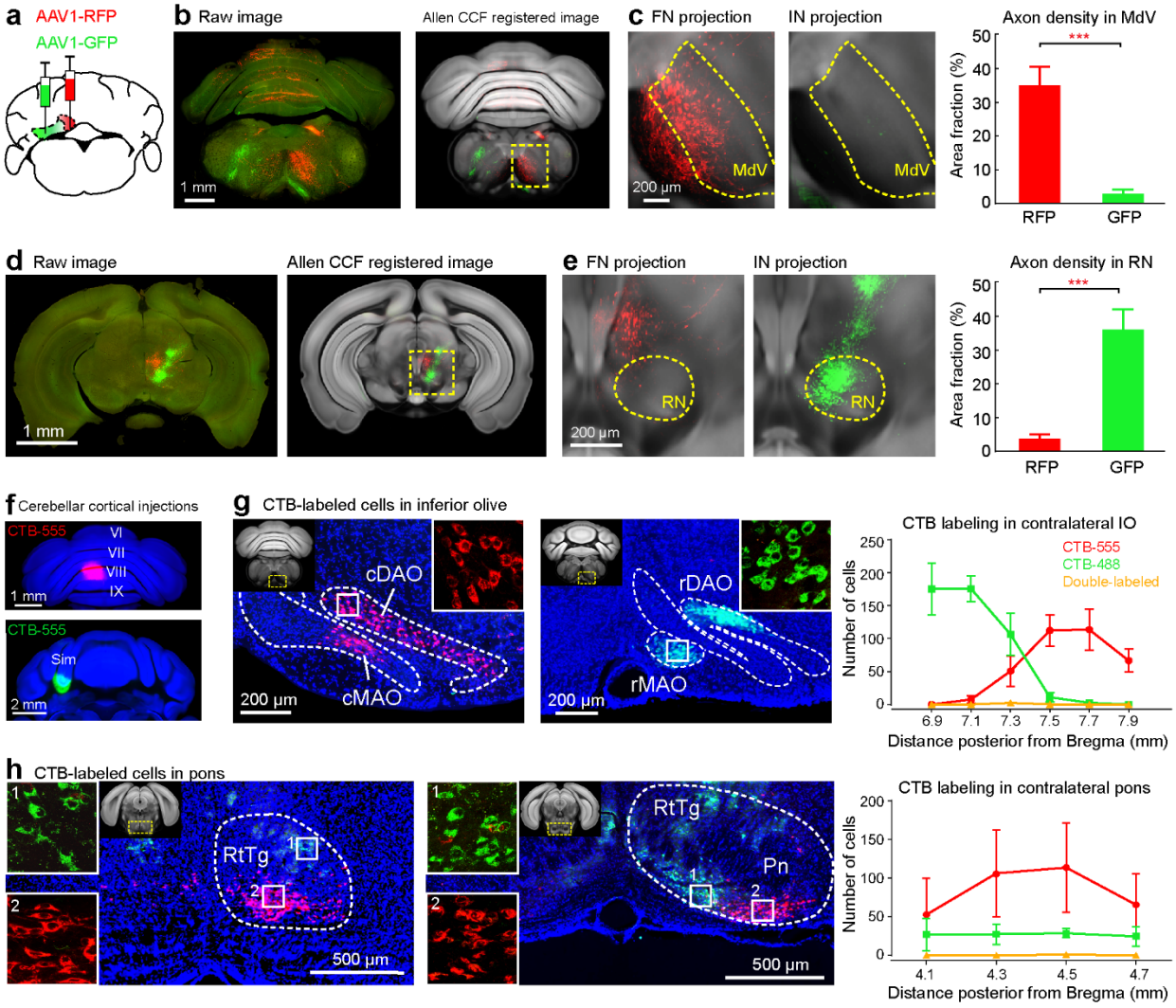

Supplementary Figure 10. Inputs and outputs of the simplex lobule-IN and the vermis-FN modules. Data related to Fig. 8

a, Tracing strategy to label FN (AAV1-RFP) and IN (AAV1-GFP) output projections. **b**, Coronal sections showing an example case of IN and FN projections at the level of caudal medulla. Raw image (left) is registered to the Allen Mouse Brain CCF (right, see Methods). Zoom-in image of the dashed-lined area containing MdV region is shown in **c**. Quantification of projection from FN and IN to MdV (**c**, n = 3, paired *t*-test, ***$P < 0.001$). **d**, **e**, Same as **b**, **c**, but for projections in the RN. IN: anterior interposed nucleus; RN: red nucleus; MdV: ventral medullary reticular nucleus. **f**, Coronal sections showing an example case with double fluorescent CTB injections in the vermis (red CTB, upper) and the simplex lobule (green CTB, lower). **g**, Coronal images and quantification of retrogradely-labeled cells in the inferior olive of 3 mice. **h**, Same as **g**, but for quantification in

139 in the Pn. cMAO: caudal medial accessory olive; cDAO: caudal dorsal accessory olive; cMAO:
140 caudal medial accessory olive; rMAO: rostral medial accessory olive; RtTg: reticulotegmental
141 nucleus of the pons; Pn: pontine nucleus.

142 **Supplementary Table 1. Stereotaxic coordinates of nuclei*.**

Nuclei	AP (mm)	ML (mm)	Depth (mm)
Fastigial nucleus	2.7	0.8	2.4
Anterior interposed nucleus	2.3	2.0	2.3
Facial nucleus	1.9	1.5	4.6
Ventral medullary reticular nucleus	3.5	0.8	4.5

143 *The origin of coordinates is defined as the anterior tip of the interparietal bone. Viral/tracer
144 injection volume was 20-50 nL. AP: anterior posterior, ML: medial lateral